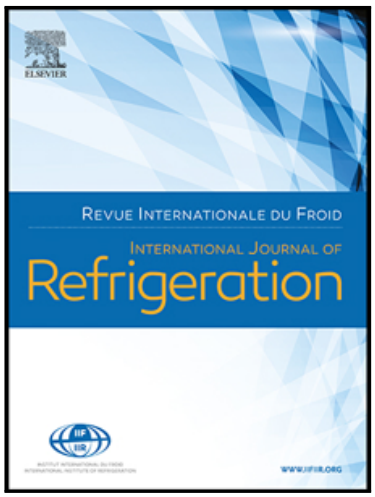

Measurement and modelling of the thermodynamic properties of carbon dioxide mixtures with HFO-1234yf, HFC-125, HFC-134a, and HFC-32: vapour-liquid equilibrium, density, and heat capacity

Arash Arami-Niya , Xiong Xiao , Saif Al Ghafri , Fuyu Jiao , Martin Khamphasith , Ehsan Sadeghi Pouya , Mirhadi Seyyedsadaghiani , Xiaoxian Yang , Tomoya Tsuji , Yukio Tanaka , Yoshio Seiki , Eric F. May

PII: S0140-7007(20)30209-7
DOI: https://doi.org/10.1016/j.ijrefrig.2020.05.009
Reference: JIJR 4774

To appear in: *International Journal of Refrigeration*

Received date: 19 February 2020
Revised date: 1 May 2020
Accepted date: 12 May 2020

Please cite this article as: Arash Arami-Niya , Xiong Xiao , Saif Al Ghafri , Fuyu Jiao , Martin Khamphasith , Ehsan Sadeghi Pouya , Mirhadi Seyyedsadaghiani , Xiaoxian Yang , Tomoya Tsuji , Yukio Tanaka , Yoshio Seiki , Eric F. May , Measurement and modelling of the thermodynamic properties of carbon dioxide mixtures with HFO-1234yf, HFC-125, HFC-134a, and HFC-32: vapour-liquid equilibrium, density, and heat capacity, *International Journal of Refrigeration* (2020), doi: https://doi.org/10.1016/j.ijrefrig.2020.05.009

Measurement and modelling of the thermodynamic properties of carbon dioxide mixtures with HFO-1234yf, HFC-125, HFC-134a, and HFC-32: vapour-liquid equilibrium, density, and heat capacity

Arash Arami-Niya[1, 2], Xiong Xiao[1], Saif Al Ghafri[1], Fuyu Jiao[1], Martin Khamphasith[1], Ehsan Sadeghi Pouya[1], Mirhadi Seyyedsadaghiani[1], Xiaoxian Yang[1], Tomoya Tsuji[3], Yukio Tanaka[4], Yoshio Seiki[4], Eric F. May[1, *]

[1] Fluid Science & Resources Division, Department of Chemical Engineering, University of Western Australia, Crawley, WA 6009, Australia

[2] Discipline of Chemical Engineering, Western Australian School of Mines: Minerals, Energy and Chemical Engineering, Curtin University, GPO Box U1987, Perth, WA 6845, Australia

[3] Malaysia-Japan International Institute of Technology, Universiti Teknologi Malaysia, Kuala Lumpur 54100, Malaysia

[4] Chemical Research Department, Research & Innovation Center, Mitsubishi Heavy Industries, Ltd., Nagasaki 851-0392, Japan

[*] Email: eric.may@uwa.edu.au
Phone number: +61 8 6488 2954

Highlights

- *New thermodynamic data reported for mixtures of CO2 with HFCs and HFO-1234yf.*
- *Data include vapour-liquid equilibrium, density and heat capacity measurements.*
- *Accuracy of reference Helmholtz equations assessed for multi-component mixtures*
- *Performance of Helmholtz equations in NIST's REFPROP 10 software package improved*

Abstract

Measurements of the thermodynamic properties for a series of more environmentally-friendly refrigerant mixtures containing hydrofluorocarbons (HFCs), hydrofluoroolefins (HFOs), and carbon dioxide (CO_2) were conducted. These new property data help increase confidence in the design and simulation of refrigeration processes that use CO_2 + HFO + HFC refrigerant mixtures. The HFCs of interest were R32, R125, and R134a and the HFO tested was R1234yf. The measurements collected were prioritised to fill gaps in the available literature data. Vapour-liquid equilibrium plus liquid-phase density and heat capacity data were collected for different binary mixtures containing HFCs, HFOs and CO_2, with the liquid phase measurements spanning (223 to 323) K and (1 to 5) MPa. The measured data, as well as data from the literature, were then used to tune the mixture parameters in the models used by NIST's REFPROP 10 software package to improve the prediction of thermodynamic

properties for these fluids. To test the predictive capabilities of the models tuned to the binary mixtures, thermodynamic property data were also measured for four ternary mixtures and a five-component mixture of HFCs, HFOs and CO_2. The new models developed in this work significantly improved the root mean square deviations of the predicted properties for these multi-component mixtures: the most significant reductions were about a factor of two in density.

Keywords: Carbon dioxide; hydrofluoroolefins; hydrofluorocarbons; vapour-liquid equilibrium; density; heat capacity

Nomenclature

A	the GC peak area	T_{step}	temperature step of calorimetry experiment
c_p	isobaric specific heat capacity	ρ	density
N_{tuned}	number of data points used in fitting of Helmholtz model binary interaction parameters		
k	GC response factor		
p	pressure		
R	GC peaks areas ratio of 2 components	**Subscripts**	
T	temperature		
u	absolute uncertainty	c	at the critical point
x	liquid mole fraction	cal	calculated
y	vapour mole fraction	i	integer counter representing a component number in a mixture
z	overall mole fraction	j	integer counter representing a component number in a mixture
α	the relative response factor in GC calibration	liq	liquid
β_v	Helmholtz energy model binary interaction parameter	n	integer counter for data point number
β_T	Helmholtz energy model binary interaction parameter	r	relative
γ_v	Helmholtz energy model binary interaction parameter	sat	under saturation
γ_T	Helmholtz energy model binary interaction parameter	vap	vapour

1 Introduction

The global warming potential (GWP) of dominant hydrofluorocarbon refrigerants (HFCs) such as R134a motivate the search for new refrigerants with a lower effect on climate that can efficiently work in current refrigeration cycles. Hydrofluoroolefins (HFOs) are a new generation of refrigerants with a much lower global warming potential than conventional HFC refrigerants. However, the performance of HFOs in existing refrigeration cycles is generally inferior, with a higher amount of energy required for the same cooling power.

Another concern about HFOs relates to their Standard 34 classification by the American Society of Heating, Refrigerating and Air-Conditioning Engineers (ASHRAE) as "marginally flammable"[1,2]. Blending these new types refrigerants with existing ones offers a way to improve the performance and decrease the GWP of the working fluid simultaneously [3].

The low GWP and suitable phase behaviour of fluids such as carbon dioxide (R744), propane (R290), and ammonia (R717), make them promising candidates for reducing the environmental impact of industrial refrigerants. Among this class of refrigerants, R744 is more suitable for use in HFO-containing refrigerant blends because of its lower flammability and toxicity compared with R290 and R717, respectively [4, 5]. Non-ignitable HFC compounds such as R125 and R134a can also reduce the flammability of HFOs and improve the mixture's performance. Mixtures of HFOs, HFCs and CO_2 are thus promising candidates for refrigerants to be used in air conditioning and building cooling applications; these blends present high working capacity with low GWP and flammability. However, to design and simulate a refrigeration system, property data for the fluid mixtures need to be measured at relevant conditions of pressure, temperature and composition so that equations of state and transport property models can be anchored to them. Recently, Bobbo et al.[6] reviewed the state of the art for experimental thermophysical properties of low GWP halocarbon refrigerants, with May and co-workers [7, 8] subsequently reporting data and tuned Helmholtz models for binary mixtures of HFOs and HFCs. Nevertheless, still there is still a significant need for new experimental data for a wide range of both properties and conditions to tune the models used by engineers for refrigerant design and optimisation.

The current study aims to provide the reference quality thermodynamic property data for the binary, ternary and multi-component mixtures of HFO-1234yf with HFC-32, HFC-125, HFC-134a and CO_2 (R744) listed in Table 1. Vapour-liquid equilibrium, as well as density and heat capacity data in the liquid phase region of the refrigerant binaries, were measured at different temperatures and pressures. The acquired data, as well as available literature data, were then used to validate and, if required, improve the Helmholtz energy equations of state (EOS) available in the software package REFPROP 10[9]. After improvement of the model's representation of the binary systems, the predictive capability of the model for the ternary (CO_2 + R1234yf + R32) and five component (CO_2 + R1234yf + R32 + R125 + R134a) mixtures were tested against the new experimental data.

Table 1. Details of the refrigerants used in the mixtures studied.

ASHRAE Refrigerant Number	IUPAC name	Chemical formula	CAS #	Refrigerant Type	Supplier	Supplier Purity (%)
R774	Carbon dioxide	CO_2	124-38-9	Natural	Core gas	99.95
R32	Difluoromethane	CH2F2	75-10-5	HFC	Core gas	99.5
R134a	1,1,1,2-Tetrafluoroethane	CH2FCF3 	811-97-2	HFC	Core gas	99.5
R125	Pentafluoroethane	C2HF5 	354-33-6	HFC	Core gas	99.95
R1234yf	2,3,3,3-Tetrafluoroprop-1-ene	C3H2F4 	754-12-1	HFO	Core gas	99.99

2 Material and methods

2.1 Materials

The refrigerants investigated in this study and their supplied purity are given in Table 1. The reference Helmholtz-free energy equations of state (EOS) implemented in the REFPROP 10 software that were used to describe the thermodynamic properties of the pure refrigerants considered in this study are listed in Table 2. The expected uncertainties of the reference EOS for each of these various thermodynamic properties are also included in Table 2. In addition to being the basis of the mixture models, these reference EOS for the pure refrigerants were used for the necessary mixture-preparation calculations.

Table 2 Components studied in this work, sources of their pure fluid equations of state (EOSs) in the software REFPROP 10 and expected standard relative uncertainties for thermodynamic properties as indicated by summary of the original reference given in REFPROP 10.

Component	*Reference equation of state*	*Expected relative uncertainty (%)*
CO_2	Span and Wagner, 1996 [10]	ρ = 0.03-0.05 p_{sat} = 0.012 $c_{p,liq}$ = 1.5
R1234yf	Richter et al., 2011 [11]	ρ_{vap} = 0.5 ρ_{liq} = 0.1 p_{sat} = 0.1 $c_{p,liq}$ = 5
R32	Tillner-Roth and Yokozeki, 1997 [11]	ρ = 0.05 p_{sat} = 0.02 $c_{p,liq}$ = 0.5-1
R134a	Tillner-Roth and Baehr, 1994 [12]	ρ = 0.05 p_{sat} = 0.02 $c_{p,liq}$ = 0.5-1
R125	Lemmon and Jacobsen, 2005 [13]	ρ = 0.04-0.5 p_{sat} = 0.2 $c_{p,liq}$ = 0.5

Al Ghafri et al.[7] described the procedure used to volumetrically prepare and transfer binary refrigerant mixtures into various apparatus that were also used here for the density and heat capacity measurements. In summary, the procedure consisted of transferring measured amounts of each pure component from one high-pressure syringe pump into another high-pressure syringe pump that also contained a mixing capability. Once all the components had been loaded, they were then mixed at high-pressure (5 MPa) under liquid phase conditions. This homogenous liquid mixture was then transferred into the apparatus at constant pressure by first back-filling and pressurising (to 5 MPa) the apparatus and lines connecting it to the mixing pump with a pure component contained in a third syringe pump. The mixing pump was then used to displace the pure component with the synthetically prepared mixture by injecting at a fixed, slow flow rate while the third syringe pump was maintained the system pressure by withdrawing the pure component as the mixture was injected. To ensure any impact on the composition of the mixture in the apparatus was negligible, the displaced volume was at least several times that of the apparatus volume. Specific details of the syringe pump arrangements and connections to the various apparatus are shown in Sections 2.3 and 2.4.

The formula provided by Al Ghafri et al.[7] for estimating the standard mole fraction uncertainty $u(x_i)$ of each component in the synthetic binary is extended here to the general case of a multi-component mixture preparation. For component i in an N component mixture, the standard uncertainty in the mole fraction of x_i is given by

$$u(x_i) = x_i(1-x_i)\sqrt{u_r(n_i)^2 + u_r(N_k)^2}, \text{ where } N_k = \sum_{j \neq i} n_j \quad (1)$$

Here u_r denotes the standard relative uncertainty of a quantity and n_i is the molar amount of component i added to the mixture. From eq (1) it apparent that in general, the uncertainty in x_i depends on the uncertainties in the amounts of all the components added to the mixture. For the special case of the binary mixture, it can be shown that eq (1)implies $u(x_1) = u(x_2)$. However for a multi-component mixture, each component's mole fraction has an uncertainty that differs from those of the other components. For example, a ternary mixture with components i, p and q has $u(x_i)$ given by

$$u(x_i) = x_i(1-x_i)\sqrt{u_r(n_i)^2 + \left(\frac{n_p}{n_p+n_q}\right)^2 \cdot u_r(n_p)^2 + \left(\frac{n_q}{n_p+n_q}\right)^2 \cdot u_r(n_q)^2} \quad (2)$$

In this work, the uncertainties in the amounts of each component transferred into an apparatus arise principally from the uncertainties in displacement volumes measured by the syringe pumps used in the preparation process.

2.2 Vapour-liquid equilibrium

2.2.1 Apparatus Overview

The vapour-liquid equilibrium (VLE) apparatus employed in this study is illustrated in Figure 1. Two systems (called System 1 and System 2 henceforth) were used in parallel to improve the data collection rate. System 1 and System 2 shared one gas chromatograph (GC, Agilent 7890A) and were otherwise fundamentally the same as the system described by May and co-workers[7 14]. The main difference between the current set-up and those detailed previously was the use of a thermal conductivity detector (TCD) instead of a flame ionization detector for the GC measurements. The VLE cells were placed in Memmert ovens (UN110) with a normal operating temperature range from 5 °C above ambient to 300 °C. To achieve lower temperatures, a copper plate-spiral tubes-plate was designed, positioned under the cells and connected to refrigerated circulators following an approach to that of Efika et al. [15]. Two fans inside the ovens were also responsible for circulating the air, thereby making the temperature profile more uniform.

For the VLE experiments, a capillary column (Agilent J&W HP/PLOT-U) was used to separate the components of the sample and adjust the requisite retention time between the GC peaks for most of the mixtures, except for five-component mixture and binary mixture of R32 + CO_2. In those cases, a packed column (Shinwa Express Sunpak-H 80/100 Glass) was

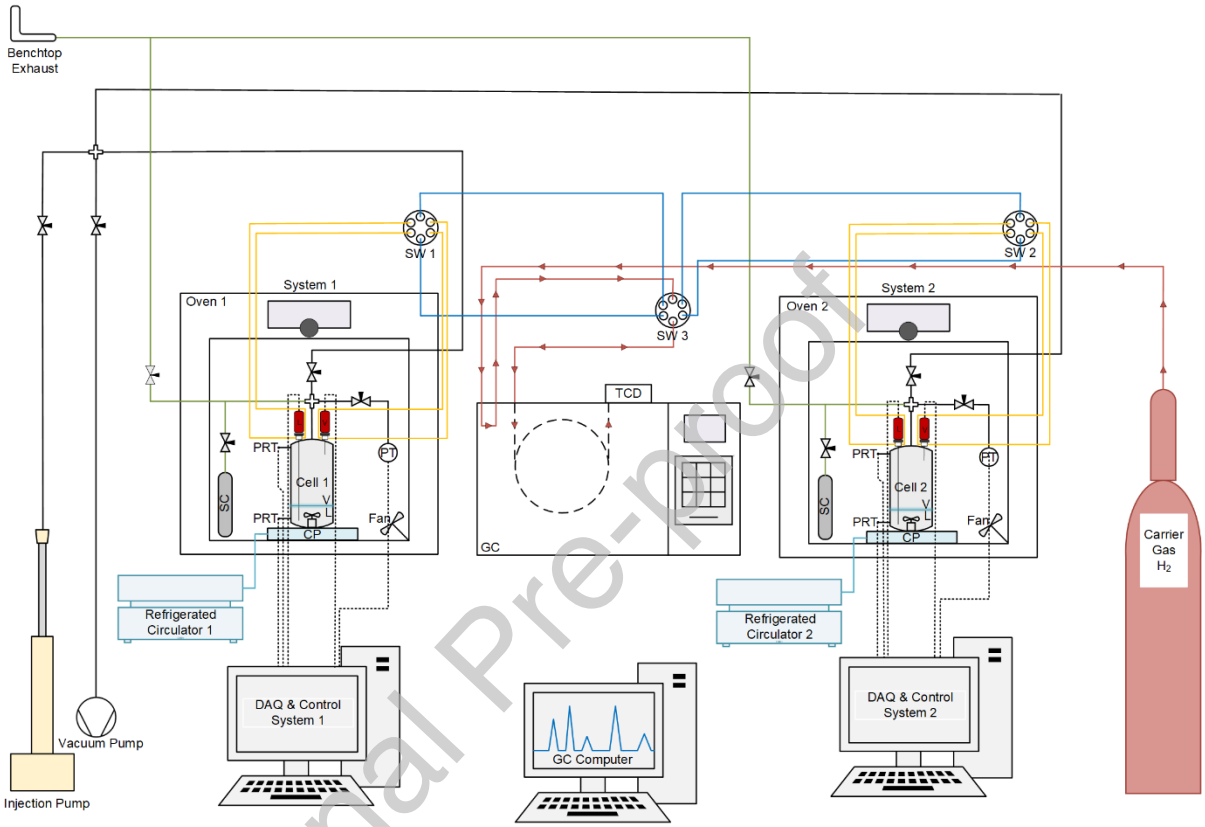

Figure 1. Schematic diagram of the VLE apparatus (CP: Cooling plate; DAQ: Data acquisition; GC: Gas chromatograph, PRT: Platinum resistance thermometer; SC: Sample cylinder; SW: Switch valve; TCD: Thermal conductivity detector). SW 3 was used to shift from Cell 1 to Cell 2 (or vice versa). SWs 1 and 2 were used to shift from the vapour ROLSI® sampler[16, 17] to the liquid ROLSI® sampler (or vice versa) for each cell.

employed to improve separation of the components.

2.2.2 GC Calibration

To calibrate the GC, binary mixtures of the refrigerants with CO_2 as the common compound (i.e., CO_2 + the other refrigerant), were volumetrically prepared at different ratios in sample cylinders. Additionally, for the 5-component experiments, two ternary mixtures with R125 as the common compound (CO_2 + R32 + R125 and R134a + R1234yf + R125) were volumetrically prepared at different concentrations of the components. The exact composition of the prepared calibration mixtures was gravimetrically determined, as described in the Supporting Information section.

Each calibration mixture was transferred to the VLE cell after it was heated to the temperature at least 10 K above the mixture's calculated cricondentherm (T_{Heated}) to make sure there was only one phase in the cylinder. The VLE cell was also heated to T_{Heated} and after reaching a stable temperature and pressure, samples were taken from the single-phase mixture. Different opening times of the ROLSI® IV electromagnetic sampling valve [16,17] were selected to ensure that a broad enough range of GC peak areas was covered.

The average of the peak areas obtained for each component, A_i, were combined in a ratio A_i / A_j and plotted against the known mole fraction ratio z_i / z_j. The calibration data were fitted to a linear equation with the intercept constrained to zero:

$$(z_i/z_j) = k_{ij} \times (A_i/A_j) \quad (3)$$

where k_{ij} denote the relative response factor for the two compounds. In eq (3), component j was CO_2 for binary and ternary experiments, while it was R125 for the 5-component experiments. To convert the integrated GC peak areas to mole fractions, eq (3) and the normalisation requirement, $\sum_{i=1}^{n} z_i = 1$, were solved simultaneously.

The GC calibration results (Figures S1 and S2 of the SI), the details of the GC temperature programs for the GC calibration and the VLE experiments (Table S1), and the relative response factors (Table S2) are reported in the Supporting Information.

2.2.3 Measurement procedure

After evacuating the VLE cell and the connection lines, the predetermined volumes of the pure refrigerant(s) were injected to the cell separately to achieve a target overall mixture composition. Then the cell was heated in the oven to a temperature 10 K above the predicted critical temperature of the injected mixture while the stirrer was on to produce a homogenous one-phase mixture. The overall composition of the mixture was confirmed by analysing samples taken from the top and bottom of the cell while it was still at the supercritical temperature. Then the oven's temperature was set to the desired measurement temperature with the stirrer on. Upon reaching an equilibrium condition, the vapour and liquid phases were sampled and the composition of each phase was determined by the GC.

2.2.4 Uncertainty calculation:

The method used for the uncertainty estimation is similar to our previously reported method[7]. The only minor change was use of a relative calibration instead of an absolute calibration for the GC's detector response. The combined uncertainty in the mole fraction is the sum of the

contributions of the uncertainty in the temperature, pressure, GC's detector response factor and the area ratios used to determine each component molar fractions. Hence the following can be written for a binary system:

$$u^2(x_i) = \left(\frac{\partial x_i}{\partial T}\right)^2 u(T)^2 + \left(\frac{\partial x_i}{\partial p}\right)^2 u(p)^2 + \left(\frac{\partial x_i}{\partial k_{ij}}\right)^2 u\left(k_{ij}\right)^2 + \left(\frac{\partial x_i}{\partial R_{ij}}\right)^2 u\left(R_{ij}\right)^2 \qquad (4)$$

Here k_{ij} is the chromatographic response factor and $R_{ij} \equiv (A_i / A_j)$ is the area ratio of the chromatographic peaks for component i and component j. The uncertainty of the mole fraction arising from the peak area ratios and the detector calibration factor were determined from the standard deviation of the peak area ratios obtained during sampling, the uncertainties during calibration of both the peak area ratios, and the uncertainties of the measured pure substance masses from the gravimetric preparation. Although the manufacturer reported uncertainties for the PRTs and pressure transducers were 0.02 K and 0.01% of the full-scale range (13.8 MPa), respectively, the thermal stability of the ovens meant these were increased to 0.1 K and 0.005 MPa, respectively.

2.3 Density method

2.3.1 Apparatus overview and experimental procedure

The density measurements were conducted with a commercial, high-pressure vibrating tube densimeter[7] (VTD), (Anton Paar, DMA HPM). The experimental setup was as described previously[7] except that the temperature control system was upgraded to a Weiss Environmental Chamber with a working temperature range of (203.15 to 453.15) K. A schematic of the entire system is shown in Figure 2.

Before loading the mixtures prepared in ISCO Syringe Pump 1, the system up to V0 (Figure

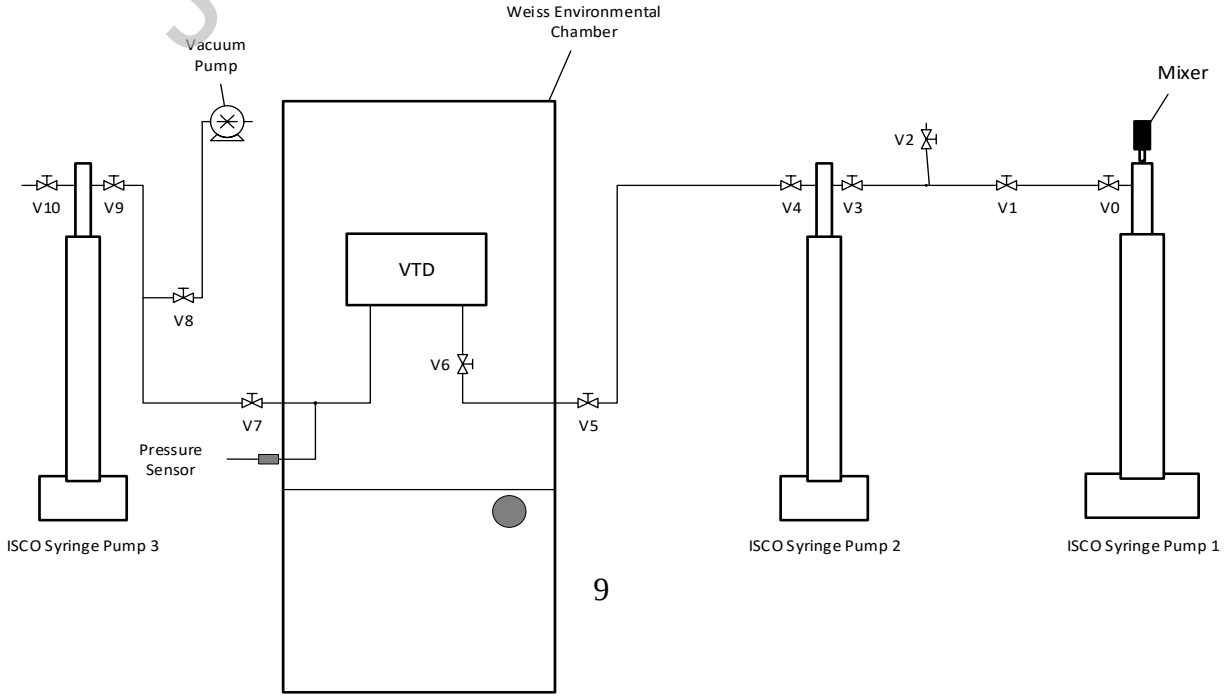

Figure 2. Schematic diagram of the VTD assembly.

2) was flushed at least 3 times, evacuated and then pressurized with pure CO_2 to above the mixture's saturation pressure using ISCO Syringe Pump 3, with ISCO Syringe Pump 2 in an empty condition (minimum volume). To displace the mixture through the VTD and avoid any phase change or fractionation, ISCO Syringe Pump 3 was set in constant pressure mode, ISCO Syringe Pump 1 was placed in constant flow mode and set to a low flow rate (1 ml·min^{-1} or less), and valve V0 was opened. The displacement of the refrigerant mixture continued until at least three times the total volume of the VTD and transfer lines (V ≈ 10 ml) had been injected from ISCO Pump 1.

Once the displacement process was completed, V7 was closed and ISCO Pump 2 was set to refill at the same flowrate as ISCO Syringe Pump 1 (1 ml·min^{-1} or less) until the desired volume of mixture had been transferred into ISCO Syringe Pump 2. Then, V3 was closed and ISCO Syringe Pump 2 was set to constant pressure mode at the desired pressure for a few hours allowing the mixture inside the VTD to stabilize before the measurement was recorded.

The calibration of the VTD was extended to lower temperatures than previously reported for such instruments [18], and is detailed further by Jiao et al.[19]. The VTD was connected to a system controller (Anton Paar, Davis5) which displayed the measured parameters including the pressure, p temperature and the tube's resonant period of oscillation (τ). These quantities were used to calculate the fluid mixture density (ρ_F) according to the model described by May et al. [20]:

$$\rho_F = \frac{(\rho_M / S_{00})}{(1+\alpha_V t+\beta_V p)} \times \left(\left(\frac{\tau}{\tau_{00}(1+\varepsilon_{\tau 1} t+\varepsilon_{\tau 2} t^2)}\right)^2 (1+\beta_\tau p) - 1\right) \quad (5)$$

Here t is the difference between the system temperature and a selected reference temperature (273.15 K); S_{00} is the geometric sensitivity factor of the evacuated tube at the reference temperature; τ_{00} is the resonance period of the evacuated tube at the reference temperature; $\varepsilon_{\tau 1}$ and $\varepsilon_{\tau 2}$ are the linear and quadratic temperature response coefficients of the spring constant, respectively; β_τ is the pressure response coefficient of the spring constant; and α_V and β_V are the linear temperature response and pressure response coefficients of tube volume, respectively.

The three parameters describing the vacuum resonance and its variation with temperature, τ_{00}, $\varepsilon_{\tau 1}$ and $\varepsilon_{\tau 2}$ were determined by linear least squares regression to data measured with the

evacuated VTD while the remaining four parameters were determined by regression of pure methane and propane data measured over a wide range of pressure and temperature conditions, as shown in Figure S3 of the SI. The relative deviations between the fitted values and those predicted by the corresponding reference EOS implemented in REFPROP 10[21, 22] were between (-0.5 to 0.5) kg·m^{-3}, respectively, which is excellent considering the wide temperature range considered in the calibration.

2.3.2 Uncertainty calculation

The combined standard uncertainty in density is estimated by (Eq. 6):

$$u^2(\rho) = \underbrace{\left\{ \begin{array}{l} (\frac{\partial \rho}{\partial S_{00}})^2 u^2(S_{00}) + (\frac{\partial \rho}{\partial \alpha_V})^2 u^2(\alpha_V) + (\frac{\partial \rho}{\partial \beta_V})^2 u^2(\beta_V) \\ +(\frac{\partial \rho}{\partial \tau_{00}})^2 u^2(\tau_{00}) + (\frac{\partial \rho}{\partial \varepsilon_{\tau 1}})^2 u^2(\varepsilon_{\tau 1}) + (\frac{\partial \rho}{\partial \varepsilon_{\tau 2}})^2 u^2(\varepsilon_{\tau 2}) + (\frac{\partial \rho}{\partial \beta_\tau})^2 u^2(\beta_\tau) \end{array} \right\}}_{Calibration}$$
$$+ \underbrace{\left\{ (\frac{\partial \rho}{\partial p})^2 u^2(p) + (\frac{\partial \rho}{\partial t})^2 u^2(t) + (\frac{\partial \rho}{\partial \tau})^2 u^2(\tau) \right\}}_{Measurement} + \underbrace{\left\{ (\frac{\partial \rho}{\partial x})^2 u^2(x) \right\}}_{Composition} \quad (6)$$

The variables that contribute primarily to the overall uncertainties in the density measurements are uncertainties associated with calibration and the reproducibility of the measured period of oscillation. The effect of the temperature, pressure and mixture composition uncertainties on the density measurements were also considered when evaluating the combined uncertainty. The relative standard uncertainty associated with the calibration was estimated to be 0.3 %, based on the calibration and validation measurements conducted with pure methane and pure propane.

Partial derivatives of pressure and temperature were estimated using REFPROP 10[9]. The overall standard uncertainty of the cell temperature was estimated to be 0.1 K, taking into account temperature gradients and fluctuations, while the global standard uncertainty of the pressure measurement was estimated to be 0.01 MPa. The uncertainty in density attributed to the measured period of oscillation, τ, was estimated to be the difference between the density of the mixture calculated with exact measured period of oscillation, τ, and that calculated with $\tau+u(\tau)$; the standard uncertainty of the measured period of oscillation, $u(\tau)$, was previously estimated to be 0.02 μs [7] . The uncertainty in density due to the uncertainty in the composition of the sample was estimated to be the difference between the density of the mixture with the specified composition and that varied by its standard uncertainty, as estimated using the default models in REFPROP 10.[9] Equation (1) was used to estimate the

standard uncertainties of the mixture mole fractions, which were 0.005 for the equimolar binary mixtures considering the contributions to the uncertainties in the amounts of each component added due to fluid injection, mixture preparation, mixture transfer, mixture purity and homogeneity. Taking all of this into account, the combined standard relative uncertainty of the measured densities ranges between (0.30 and 0.45) %, as shown Figure S4 of the SI for all mixtures; the primary contribution to the final uncertainty being the quality of the calibration.

2.4 Isobaric heat capacity method

2.4.1 Apparatus overview and experimental procedure

Isobaric heat capacities, c_p, were measured via a commercialised differential scanning calorimeter (Setaram DSC BT 2.15) described previously.[7] For this work, liquid nitrogen was used instead of water as a coolant to cover the required temperature range of the measurements. Refrigerant mixtures were loaded into the DSC following the procedure described by Al Ghafri et al.[7] Pure CO_2 was used to backfill the DSC measurement cell up to valve 7 in Figure 3, at a pressure of 10 MPa or more. To flush the mixture through the cell, pump 2 was set to maintain constant pressure (10 MPa). ISCO Pump 1 (Floxlab, BTs605/606-0 / SS / 500cc / SN 4342) was then set to constant flow mode at a low flow rate (2 ml·min^{-1} or less) and valves 7 and 8 were simultaneously opened. This ensured the displacement of the mixture through the DSC cell without any inadvertent phase change, thereby avoiding fractionation of the mixture. The displacement continued until at least 40 ml of volume passed through the cell, which is much larger than the volume of the DSC cell (≈ 9 ml). Once the displacement process was complete, valve 2 was closed and pump 1 was set to constant pressure mode at the desired pressure of the measurement.

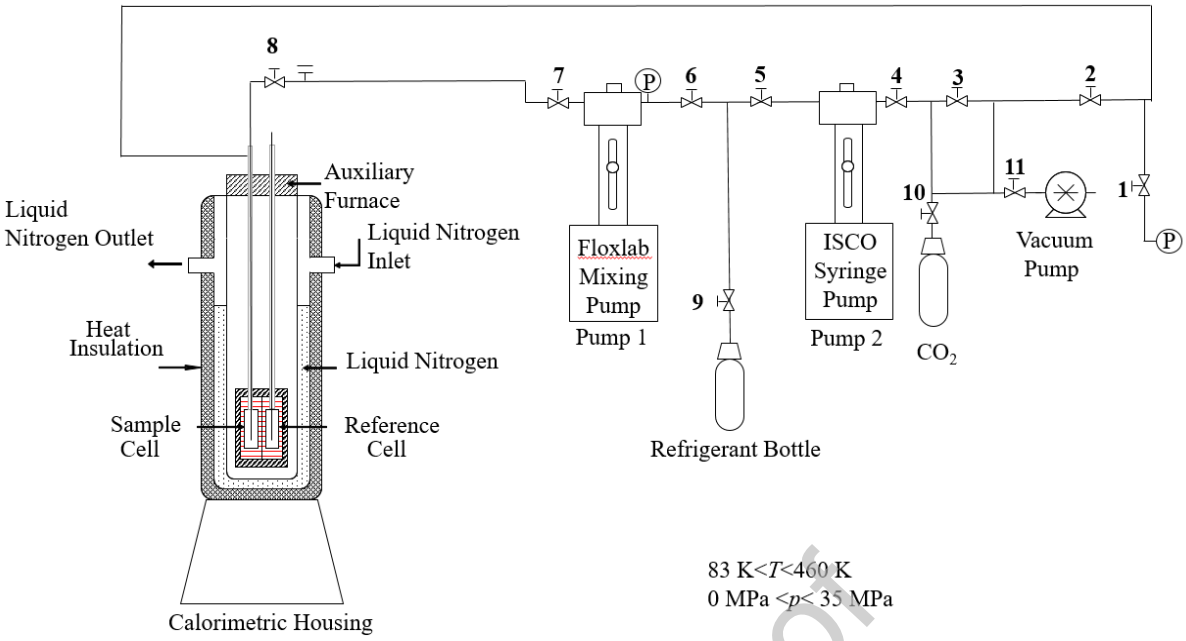

Figure 3. Differential scanning calorimeter (Setaram DSC BT 2.15) used for measurements of the isobaric heat capacity of refrigerant mixtures.

The isobaric heat capacity was measured by the step method with the DSC's reference cell filled with dry nitrogen at atmospheric pressure. Following an initial isothermal equilibration period of 4 h, the DSC furnace temperature was increased by 10 K at a constant rate of 0.15 K·min^{-1}. A final isothermal period of 6 h followed the temperature ramp. To account for the heat capacity of the DSC cell itself, a series of blank experiments with dry nitrogen gas under atmospheric pressure in the measurement cell were also performed. The isobaric heat capacities were then calculated from

$$c_p = \frac{\int \Phi_s \mathrm{d}t - \int \Phi_b \mathrm{d}t}{\rho V_{\mathrm{cell}} \Delta T_{\mathrm{step}}} \qquad (7)$$

where $\int \Phi_s \mathrm{d}t$ is the integrated heat flow difference between the measurement cell filled with sample and the reference cell containing dry N_2 at atmospheric pressure over the temperature step (scan), $\int \Phi_b \mathrm{d}t$ is the integrated heat flow difference for the calibration scans where both the measurement and reference cells were filled with dry N_2, ρ is the fluid density (tuned in this work for the refrigerant mixtures), V_{cell} is the volume of the cell and ΔT_{step} is the temperature step (10 K). The volume of the cell was determined to be (8.947 ± 0.043) cm^3 using propane at a pressure of 2 MPa as a reference fluid.

2.4.2 Uncertainty calculation

The uncertainty of a heat capacity measurement was estimated via the GUM method[23] from the following equation:

$$u^2(c_p) = \sum_{i=1}^{n}\sum_{j=1}^{n}\frac{\partial f}{\partial y_i}\frac{\partial f}{\partial y_j}u(y_i, y_j) \tag{8}$$

where y_i and y_j are the input variables, $(\partial f/\partial y_i)$ is the sensitivity coefficient for y_i, $u(y_i, y_j)$ is the covariance ($i \neq j$) or the variance ($i = j$) of variables y_i and y_j, and $u^2(y)$ is the variance of y.

The measurement of heat capacity is also dependent on temperature, pressure and mixture composition. With $Q = \int \Phi_s \mathrm{d}t - \int \Phi_b \mathrm{d}t$, eq (8) becomes:

$$u^2(c_p) = \left(\frac{\partial c_p}{\partial Q}\right)^2 u^2(Q) + \left(\frac{\partial c_p}{\partial \rho}\right)^2 u^2(\rho) + \left(\frac{\partial c_p}{\partial V}\right)^2 u^2(V) + \left(\frac{\partial c_p}{\partial \Delta T}\right)^2 u^2(\Delta T) + \left(\frac{\partial c_p}{\partial T}\right)^2 u^2(T) + \left(\frac{\partial c_p}{\partial p}\right)^2 u^2(p) + \left(\frac{\partial c_p}{\partial x}\right)^2 u^2(x) \tag{9}$$

where $\frac{\partial c_p}{\partial Q} = \left(\frac{1}{V\rho\Delta T}\right)^2$, $\frac{\partial c_p}{\partial V} = \left(\frac{Q}{V^2\rho\Delta T}\right)^2$, $\frac{\partial c_p}{\partial \rho} = \left(\frac{Q}{\rho^2 V\Delta T}\right)^2$, and $\frac{\partial c_p}{\partial \Delta T} = \left(\frac{Q}{\Delta T^2 V\rho}\right)^2$, and $u_B(c_p)$ is any Type-B uncertainty. The Type-B uncertainty is an estimate of the systematic uncertainty compared with independent measurements or a well-defined equation of state of lower uncertainty as discussed by Tay and Trusler[24]. In this work, pure methane [25] was measured for the validation of the Type-B uncertainty with a Helmholtz energy EOS from Setzmann and Wagner[22]. No systematic error was observed and thus the Type-B uncertainty was taken to be negligible. For each term in eq (9), a summary of the method of estimation and a representative value are listed in Table 3.

Table 3 List of the estimation method and representative values for the uncertainties and the derivative terms in eq (9).

Term	Estimation method	Value
$u(Q)$	The standard deviation of Joule-effect	0.30 J

	calibration measurement from the fitted 4th polynomial curve	
$u(\rho)$	The estimated uncertainty in the new regressed equation of state	$0.5\% \cdot \rho$
$u(V)$	The standard deviation in the three effective cell volume measurements	0.028 mL
$u(\Delta T)$ and $u(T)$	The standard deviation for temperature in the melting point measurement	0.15 K
$u(p)$	Combined from pressure stability in the measurement and the pressure transducer calibration	$\sqrt{\left(0.005 \cdot \left(\frac{p}{\text{MPa}}\right)\right)^2 + 0.005^2}$ MPa
$u(x)$	Combined from all the factors in the fluid injection, mixture preparation, density obtained from REFPROP 10, mixture transfer and mixture homogeneity	0.005
$\frac{\partial c_p}{\partial T}$, $\frac{\partial c_p}{\partial p}$ and $\frac{\partial c_p}{\partial x}$	Estimated by the EOS implemented in REFPROP 10	
$u_B(c_p)$	The systematic uncertainty of pure methane measurements compared with the reference equation of state	0

2.5 Helmholtz energy mixture model

The state-of-the-art approach for predicting the thermodynamic properties of refrigerant mixtures is based on fundamental Helmholtz equations of state. As part of this work, the capability of existing models to predict the experimentally-determined data for refrigerant mixtures was assessed, and then these models were tuned to data available for binary mixtures where applicable. The multi-component mixture data were used to verify the predictions of the models with the tuned binary interaction parameters.

The mixing rules for Helmholtz equations describing refrigerant mixtures are the same as those utilized in the GERG-2008 EOS.[26] To describe binary mixture thermodynamic properties, reducing functions containing binary interaction parameters are used to tune to available experimental data:

$$\frac{1}{\rho_{c,ij}} = \beta_{v,ij}\gamma_{v,ij}\frac{x_i+x_j}{\beta_{v,ij}^2 x_i + x_j} \cdot \frac{1}{8}\left(\frac{1}{\rho_{c,i}^{1/3}} + \frac{1}{\rho_{c,j}^{1/3}}\right)^3 \quad (10)$$

$$T_{c,ij} = \beta_{T,ij}\gamma_{T,ij}\frac{x_i+x_j}{\beta_{T,ij}^2 x_i + x_j}\left(T_{c,i}T_{c,j}\right)^{1/2} \quad (11)$$

The parameters $\rho_{c,i}$ and $T_{c,i}$ are the critical density and critical temperature of pure fluid i, $\beta_{v,ij}$, $\gamma_{v,ij}$, $\beta_{T,ij}$ and $\gamma_{T,ij}$ are binary interaction parameters (BIPs) between fluids i and j, and x_i is the mole fraction of component i in the mixture. The BIPs can be set to unity for binaries with very few or no data. In cases where large numbers of accurate data are available or the BIPs alone cannot describe the available thermodynamic data well, a departure function (linked with an adjustable factor, F_{ij}) might be used. Mixtures with more than 2 components are calculated using the binary interaction models with no further terms incorporated.

In this work, only the binary interaction parameters within the reducing functions were tuned; no departure functions were adjusted. The binary interaction parameters were tuned by minimising the root mean square (RMS) deviations between the selected experimental data and the model. The RMS deviations were calculated via the following equations for the three types of thermodynamic properties considered:

$$\mathrm{RMS(VLE)} = \left(\frac{1}{N}\sum_{n=1}^{N}\left[\left(x_{1,n} - x_{1,\mathrm{calc},n}\right)^2 + \left(y_{1,n} - y_{1,\mathrm{calc},n}\right)^2\right]\right)^{\frac{1}{2}} \quad (12)$$

$$\mathrm{RMS}(\rho) = 100\left(\frac{1}{N}\sum_{n=1}^{N}\left(\frac{\rho_n - \rho_{\mathrm{calc},n}}{\rho_n}\right)^2\right)^{\frac{1}{2}} \quad (13)$$

$$\mathrm{RMS}\left(c_p\right) = 100\left(\frac{1}{N}\sum_{n=1}^{N}\left(\frac{c_{p,n} - c_{p,\mathrm{calc},n}}{c_{p,n}}\right)^2\right)^{\frac{1}{2}} \quad (14)$$

where x_1 and y_1 are the mole fraction of component 1 in the liquid and in the vapour at equilibrium, respectively. Values of x_i and y_i were obtained from the specified overall composition of the mixture z_i by calculating the properties of the equilibrium liquid and vapour phases, respectively, at the experimental temperature and pressure (flash calculation).

In this work the number of thermodynamic data available for a given binary mixture was limited. Thus, it was only necessary to tune two BIPs from their standard value (unity) to achieve acceptable fits to the data. Weighting factors were given to different properties following a method similar to that detailed by Kunz et al.[27]. The tuning procedure minimised the following objective function

$$\chi^2 = W_1\mathrm{RMS(VLE)}^2 + W_2\mathrm{RMS}(\rho)^2 + W_3\mathrm{RMS}\left(c_p\right)^2 \quad (15)$$

where W_1 to W_3 are the weighting factors applied to the different properties as considered in eqs (12)-(14). The values of the weighting factors are empirical and are determined by the

scale of the RMS deviation, the uncertainty of the experimental data, and the importance (or sensitivity) of each property. The tuning of each binary used slightly different weighting factors according to the available data situation but typically W_2 was 2-5 times larger than W_1 and 5-10 times larger than W_3. This reflects the fact that density data have the both the smallest uncertainty and the greatest influence on EOS tuning [28]. Heat capacity data have relatively large uncertainties and limited influence on EOS predictions, although they can provide good checks of mixing rule formulations as demonstrated by Syed et al.[29] and Rowland et al. [30]

For completeness, we note that Jaubert and co-workers [31] recently added six fluorinated groups to the well-known Enhanced-PPR78 model [32] allowing for the estimation of the temperature-dependent binary interaction parameters $k_{ij}(T)$ in the Peng-Robinson equation of state. While not as accurate as Helmholtz models that are adequately anchored to experimental data, the group-contribution approach allows for the prediction of the phase behaviour and thermodynamic properties for systems that are not yet measured and can thus be extremely useful to the design of very new processes and/or products. It would be interesting to apply and compare the recent extension of this group contribution scheme to the prediction of the mixture properties measured in this work.

3 Results

3.1 Experimental measurements

The experimental data measured in this work are presented in both Tables and Figures either in this Section or in the Supporting Information.

3.1.1 Vapour-liquid equilibrium

Measurement of four binary systems of (CO_2 + R32), (CO_2 + R134a), (CO_2 + R1234yf), and (CO_2 + R125) were made at constant temperatures around 293 K. Five different composition of CO_2 from (8 to 81)% were studied in each binary system. After the preparation of each mixture, the overall composition of the mixture was examined at a temperature at least 10 K above the mixture's calculated cricondentherm to ensure the presence of a single phase. For the isothermal measurements, the mixture was stabilized at a temperature of around 293 K and then the composition of the vapour (y_i) and liquid (x_i) phases were measured by sampling each more than ten times, with the average reported here. The initial composition, the saturation pressure (P^{sat}) and the equilibrium liquid and vapour compositions (x, y) for each binary at the experimental temperature (T) are listed in Table S3 of the SI. The (P-x,y) phase

envelopes of the binary mixtures are presented in Figure 4 (a) –(d), where the mole fraction of CO_2 (1) in the liquid, x_1, and vapour phases, y_1, respectively, are plotted versus the saturation pressure.

The results were compared to values reported in the literature and those that are calculated with the default Helmholtz equation of state (EOS) as implemented in REFPROP 10[9], based on the experimental pressure, temperature and overall composition using the method described by May et al. [14]. The deviations between the data and model predictions are shown in the form of mole fraction deviation plots in Figure S7 to Figure S10 of the SI. In these plots, the abscissa is the measured saturation pressure and the ordinates are the deviation of the measured mole fraction of CO_2 ($x_{1,exp}$, $y_{1,exp}$) from the value calculated with the default Helmholtz equation of state (EOS) for that component ($x_{1,cal}$, $y_{1,cal}$).

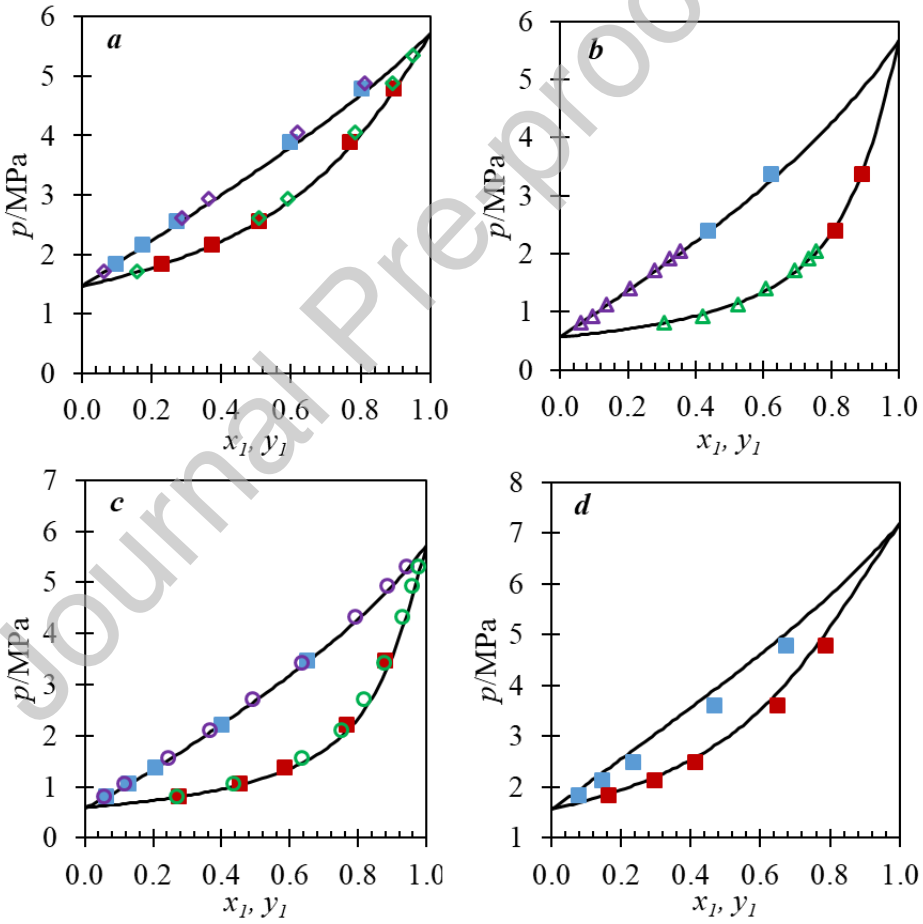

Figure 4. VLE results and phase envelope of (***a***) CO_2 (1) + R32 (2) at 292.98 K, (***b***) CO_2 (1) + R134a (2) 292.88 K, (***c***) CO_2 (1) + R1234yf (2) at 293.13 K, (***d***) CO_2 (1) + R125 (2) at 302.89 K from available experimental data and the EOS in REFPROP 10[4] using the default binary interaction parameters (BIPs). Symbols refer to the measurements at different pressures, and the solid curves refer to the model predictions. Symbol list: ■ Bubble point measured in this work ■ Dew point measured in this work ◇ Bubble point from Rivollet et al.[33] ◇ Dew point from Rivollet et al.[33] Δ

Bubble point from Duran-Valencia et al.[34] Δ Dew point from Duran-Valencia et al.[34] ○ Bubble point from Juntarachat et al.[35] ○ Dew point from Juntarachat et al [35].

The ternary mixture of (CO_2 + R1234yf + R32) was prepared by the addition of CO_2 to a near equimolar mixture of R1234yf + R32 with $z_{R1234yf}/z_{R32}$=0.45. The VLE measurements were made at four different mixture compositions and two temperatures near 284 and 312 K. The results are presented in Figure 5 and Figure S11 and tabulated in Table S3 of the SI. Before commencing each measurement, the overall composition of the mixture was measured by GC at the single gas phase condition (Table S3). Similar comparisons to values calculated with the default Helmholtz EOS implemented in REFPROP 10 are shown for the ternary mixture in Figure S12 of the SI. Comparisons of the ternary mixture VLE data with predictions made using the EOS tuned to the binary data are presented in Section 3.2.2.

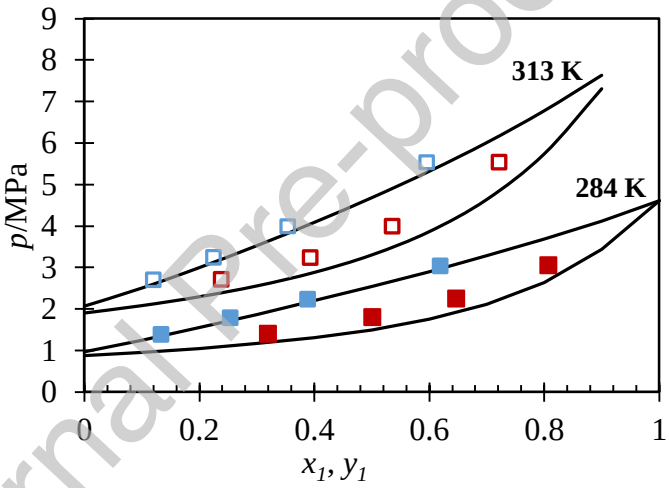

Figure 5. Measured (symbols) and predicted (curves) bubble and dew pressures at T=284 K and T=313 K for the CO_2 (1) + R1234yf (2) + R32 (3) ternary systems ($z_{R1234yf}/z_{R32}$=0.45) as a function of the measured liquid and vapour mole fractions of each component: ■ Bubble point measured in this work ■ Dew point measured in this work (filled symbols for T=284 K, and empty symbols for T=313 K) . The dew and bubble curve predictions were made with the EOS in REFPROP 10 using the default binary interaction parameters.

A near-equimolar mixture of five-components, [CO_2 (1) + R1234yf (2) + R32 (3) + R125 (4) + R134a (5)], was prepared gravimetrically then injected to the VLE cell under single-phase conditions. The overall composition of the mixture was confirmed by GC analysis. Three VLE measurements at (273, 312 and 333) K were made (Table 4) and the deviations of the results from the prediction of the default Helmholtz energy mixture model are shown in Figure 6.

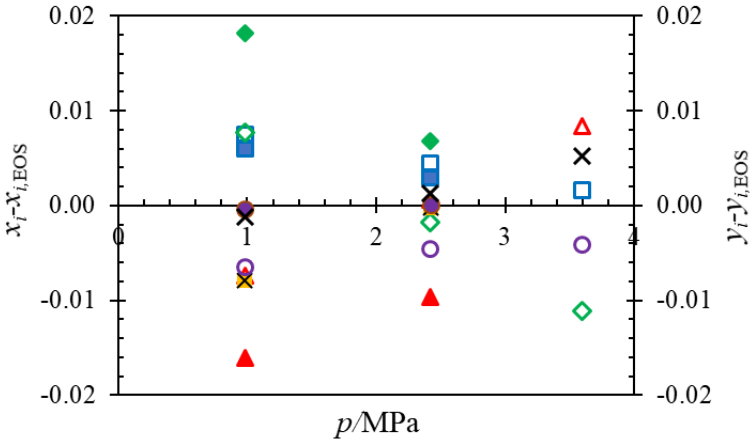

Figure 6. Deviations (x_i-$x_{i,EOS}$) and (y_i-$y_{i,EOS}$) of the measured compositions from those predicted with the default Helmholtz energy mixture model for [CO_2 (1, ◆)+ R1234yf (2, ▲)+ R32 (3, ■) + R125 (4, ●) + R134a (5, ☒)] system. Left axis: filled symbols, deviations for liquid; Right axis: empty symbols, deviations for vapour.

Table 4. Measured p,T,x,y data for a five component mixture of CO_2 (1) + R1234yf (2) + R32 (3) + R125 (4) + R134a (5) with the global composition of z_1=0.1994 ± 0.0045, z_2=0.2002 ± 0.0045, z_3=0.2015 ± 0.0045, z_4=0.2016 ± 0.0045, z_5=0.1974 ± 0.0009.

T/K	p/MPa	x_1	$u(x_1)$	y_1	$u(y_1)$	x_2	$u(x_2)$	y_2	$u(y_2)$	x_3	$u(x_3)$	y_3	$u(y_3)$	x_4	$u(x_4)$	y_4	$u(y_4)$	x_5	$u(x_5)$	y_5	$u(y_5)$
273.48	0.98	0.1812	0.0022	0.4916	0.0036	0.1974	0.0011	0.0826	0.0014	0.2066	0.0008	0.1971	0.0015	0.2068	0.0008	0.149	0.0015	0.2081	0.0012	0.0797	0.0014
312.79	2.42	0.1607	0.0055	0.3425	0.0022	0.2112	0.0055	0.1311	0.0011	0.1989	0.0054	0.2155	0.0009	0.2065	0.0005	0.1807	0.001	0.2227	0.0055	0.1303	0.0011
333.5	3.6	N/A*		0.2644	0.0018	N/A*		0.1663	0.001	N/A*		0.213	0.0008	N/A*		0.1915	0.0008	N/A*		0.1648	0.001

*At 333.5 K, a liquid phase was present but the volume available was insufficient to reliably sample and analyse its composition.

3.1.2 Density

Single-phase densities for the binary mixtures (0.50 CO_2 + 0.50 R125), (0.50 CO_2 + 0.50 R1234yf), (0.50 CO_2 + 0.50 R32), and (0.50 CO_2 + 0.50 R134a), a ternary mixture (0.09 CO_2 + 0.48 R1234yf + 0.43 R32) and a 5-component mixture (0.20 CO_2 + 0.20 R1234yf + 0.20 R32 + 0.20 R125 + 0.20 R134a) were measured at temperatures between (223 and 323) K over the pressure range of 1.0 MPa to 5.0 MPa. A total of 58 density data were acquired, ranging from (892 to 1404) kg·m^{-3}. A summary of the measurement pressure and temperature conditions is shown in Figure S5, along with the phase envelope for each mixture predicted using the default reference model implemented in the software REFPROP 10[9]. For every isotherm, density measurements were performed for a minimum duration of 3 hours at every pressure. A repetition of one pressure value was also conducted to check the measurement reproducibility.

Single-phase densities measured for the binary mixtures (0.50 CO_2 + 0.50 R32), (0.50 CO_2 + 0.50 R134a), (0.50 CO_2 + 0.50 R125) and (0.50 CO_2 + 0.50 R1234yf) at pressures between (1.5 and 5.0) MPa are shown in Table 5 and Figure S13 to Figure S16 of the SI. As an example of the binary results, Figure 7 shows (0.5 CO_2 + 0.5 R1234yf) density results and the deviations of the results from the prediction of the default Helmholtz energy mixture model. In all cases the measured values follow the same trend as the calculated values. The relative deviations between the present measurements and the values predicted with the default EOS for each system span the range (-1.77 to +1.65) %, with the relative deviations being systematically dependent on temperature.

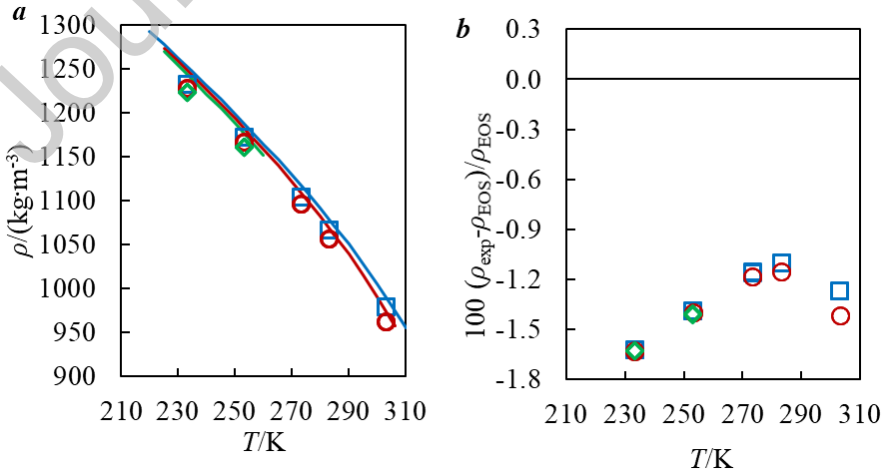

Figure 7. Comparisons of 0.5 CO_2 + 0.5 R1234yf density results for the experimental data measured in this work and various models from default binary interaction parameters (BIPs). Deviations are shown of experimental data from those calculated with the default BIPs. Symbols refer to the measurements at different pressures (□ 5.09 MPa ○ 3.56 MPa ◇ 2.04 MPa), and the solid curves refer to the model prediction.

Table 5 Measured density data for the refrigerant equimolar binary mixtures (CO_2 + R32), (CO_2 + R134a), (CO_2 + R125) and (CO_2 +R1234yf) and combined standard uncertainty $u_c(\rho)$ as a function of temperature and pressure. The standard uncertainties in the mole fractions of the binary mixtures were $u(z_1) = u(z_2) = 0.005$.

T/K	$u(T)$/K	p/MPa	$u(p)$/MPa	z_1	z_2	ρ/ kg·m^{-3}	$u_c(\rho)$/ kg·m^{-3}
CO_2 (1) + R32 (2)							
293.3	0.1	5.11	0.01	0.501	0.499	921.2	3.0
273.3	0.1	5.03	0.01	0.501	0.499	1019.5	3.2
223.3	0.1	4.98	0.01	0.501	0.499	1195.0	3.6
273.3	0.1	3.51	0.01	0.501	0.499	1012.6	3.1
253.2	0.1	3.58	0.01	0.501	0.499	1093.8	3.3
243.3	0.1	3.46	0.01	0.501	0.499	1127.8	3.4
243.3	0.1	1.26	0.01	0.501	0.499	1122.0	3.4
243.3	0.1	1.50	0.01	0.501	0.499	1123.2	3.4
223.3	0.1	1.53	0.01	0.501	0.499	1186.8	3.6
CO_2 (1) + R134a (2)							
283.3	0.1	5.05	0.01	0.500	0.500	1137.1	3.9
303.1	0.1	5.06	0.01	0.500	0.500	1045.5	3.9
253.2	0.1	3.56	0.01	0.500	0.500	1242.5	4.0
273.3	0.1	3.54	0.01	0.500	0.500	1168.4	3.9
233.3	0.1	3.98	0.01	0.500	0.500	1310.0	4.2
253.2	0.1	2.23	0.01	0.500	0.500	1238.1	4.0
233.3	0.1	2.31	0.01	0.500	0.500	1306.0	4.2
283.3	0.1	5.05	0.01	0.500	0.500	1137.1	3.9
303.1	0.1	5.06	0.01	0.500	0.500	1045.5	3.9
CO_2 (1) + R125 (2)							
293.2	0.1	5.10	0.01	0.500	0.500	1098.3	4.2
273.3	0.1	5.10	0.01	0.500	0.500	1201.9	4.2
253.1	0.1	5.06	0.01	0.500	0.500	1289.7	4.3
243.2	0.1	5.09	0.01	0.500	0.500	1328.4	4.4
223.3	0.1	5.13	0.01	0.500	0.500	1404.6	4.6
293.3	0.1	3.60	0.01	0.500	0.500	1070.1	4.3
273.3	0.1	3.59	0.01	0.500	0.500	1190.9	4.1
253.1	0.1	3.61	0.01	0.500	0.500	1283.7	4.3
243.2	0.1	3.57	0.01	0.500	0.500	1323.9	4.4
223.3	0.1	3.72	0.01	0.500	0.500	1402.6	4.5
243.2	0.1	1.41	0.01	0.500	0.500	1314.9	4.3
223.2	0.1	1.73	0.01	0.500	0.500	1396.7	4.5
223.2	0.1	1.52	0.01	0.500	0.500	1396.1	4.5
CO_2 (1) + R1234yf (2)							
303.1	0.1	5.10	0.01	0.501	0.499	978.0	3.4
283.2	0.1	5.07	0.01	0.501	0.499	1066.4	3.5
273.3	0.1	5.09	0.01	0.501	0.499	1104.2	3.5
253.2	0.1	5.08	0.01	0.501	0.499	1172.4	3.7
233.2	0.1	5.10	0.01	0.501	0.499	1233.5	3.8
303.1	0.1	3.58	0.01	0.501	0.499	961.0	3.5
283.2	0.1	3.55	0.01	0.501	0.499	1056.3	3.5
273.3	0.1	3.56	0.01	0.501	0.499	1096.1	3.5
253.2	0.1	3.58	0.01	0.501	0.499	1166.9	3.7
233.2	0.1	3.55	0.01	0.501	0.499	1229.3	3.8
253.2	0.1	2.11	0.01	0.501	0.499	1161.3	3.6
233.2	0.1	1.97	0.01	0.501	0.499	1224.8	3.8

Single-phase densities at pressures of (1.7, 3.0, and 4.5) MPa were measured for the ternary mixture (0.09 CO_2 + 0.48 R1234yf + 0.43 R32), and the data are shown in Table 6. As it was shown in Figure S17 in the SI, the measured values follow the same trend as the calculated values. The relative deviations between the present measurements and the values predicted with the default EOS span (-2.77 to -0.78) %, with the relative deviations systematically dependent on temperature.

Table 6 Measured density data for the CO_2 (1) + R1234yf (2) + R32 (3) ternary systems with the global composition of z_1=0.093 ± 0.010, z_2=0.477 ± 0.008, z_3=0.430 ± 0.009 and combined standard uncertainty $u_c(\rho)$ as a function of temperature and pressure.

T/K	$u(T)$/K	p/MPa	$u(p)$/MPa	z(CO_2)	z(R32)	z(R1234yf)	ρ/ kg·m^{-3}	$u_c(\rho)$/ kg·m^{-3}
324.1	0.1	4.53	0.01	0.092	0.434	0.474	891.1	3.7
303.5	0.1	4.53	0.01	0.092	0.434	0.474	1001.3	3.5
303.5	0.1	3.00	0.01	0.092	0.434	0.474	987.1	3.5
282.9	0.1	3.03	0.01	0.092	0.434	0.474	1070.2	3.6
275.2	0.1	3.09	0.01	0.092	0.434	0.474	1101.3	3.6
273.3	0.1	1.75	0.01	0.092	0.434	0.474	1109.6	3.6
253.2	0.1	1.70	0.01	0.092	0.434	0.474	1175.1	3.7

Single-phase densities at pressures of (1.5, 3.5 and 5.0) MPa were measured for the 5-component mixture (0.20 CO_2 + 0.20 R1234yf + 0.20 R32 + 0.20 R125 + 0.20 R134a) and the data are tabulated in Table 7 and shown in Figure S18. The measured values follow the same trend as the calculated values. The relative deviations between the present measurements and the values predicted with the default EOS span (-1.09 to -0.57)%, with the relative deviations systematically dependent on temperature.

Table 7 Measured density data for the refrigerant a five component mixture of CO_2 (1) + R1234yf (2) + R32 (3) + R125 (4) + R134a (5) with the global composition of z_1=0.200 ± 0.007, z_2=0.200 ± 0.004, z_3=0.200 ± 0.007, z_4=0.200 ± 0.005, z_5=0.200 ± 0.006. and combined standard uncertainty $u_c(\rho)$ as a function of temperature and pressure.

T/K	$u(T)$/K	p/MPa	$u(p)$/ MPa	z(CO_2)	z(R32)	z(R1234yf)	z(R134a)	z(R125)	ρ/ kg·m^{-3}	$u_c(\rho)$/ kg·m^{-3}
323.1	0.1	5.06	0.01	0.200	0.200	0.200	0.200	0.200	971.1	4.35
303.1	0.1	5.07	0.01	0.200	0.200	0.200	0.200	0.200	1079.5	3.97
283.3	0.1	5.04	0.01	0.200	0.200	0.200	0.200	0.200	1162.7	3.95
243.3	0.1	5.02	0.01	0.200	0.200	0.200	0.200	0.200	1298.8	4.14
243.3	0.1	5.07	0.01	0.200	0.200	0.200	0.200	0.200	1299.0	4.14
303.1	0.1	3.53	0.01	0.200	0.200	0.200	0.200	0.200	1065.1	4.01
283.3	0.1	3.54	0.01	0.200	0.200	0.200	0.200	0.200	1154.1	3.95
243.3	0.1	3.51	0.01	0.200	0.200	0.200	0.200	0.200	1294.3	4.13
263.2	0.1	1.43	0.01	0.200	0.200	0.200	0.200	0.200	1219.8	4.01
243.3	0.1	1.45	0.01	0.200	0.200	0.200	0.200	0.200	1287.9	4.12

3.1.3 Isobaric heat capacity

Heat capacity data for the binary refrigerant mixtures are reported in Table 8. The deviations of the measurements from the default model implemented in REFPROP 10[9] which are shown in Figure S19 to Figure S22 are within the estimated experimental uncertainties for (CO_2 + R125) and for most of the (CO_2 + R1234yf) data. Figure 8 illustrates an example of heat capacity measurements results of (0.5 CO_2 + 0.5 R1234yf) and their deviations from the REFPROP 10[1] predictions. Relatively large deviations (up to 4.9%) were observed for (CO_2 + R32) and (CO_2 + R134a). For the mixture of (CO_2 + R32), the data were all 3% higher than the predictions. All the measured data follow the same trends with temperature and pressure predicted by the default model in REFPROP 10.

For the ternary and five-component mixtures, the measured data still follow the same trend as the values predicted by REFPROP 10. The relative deviations of the experimental data from the REFPROP 10 models vary from (-4.0 to 2.0) %, which is within the experimental uncertainty for most of the points (given the increased uncertainty from the mixture composition). As shown in Figure S23 and Figure S24 of the SI, the binaries involved in these multi-component mixtures show positive and negative deviations from the default model predictions. These positive and negative differences among the different binaries mostly cancel out when the components are combined; thus, the relative deviations turn out to be relatively small for the multi-component refrigerant mixtures.

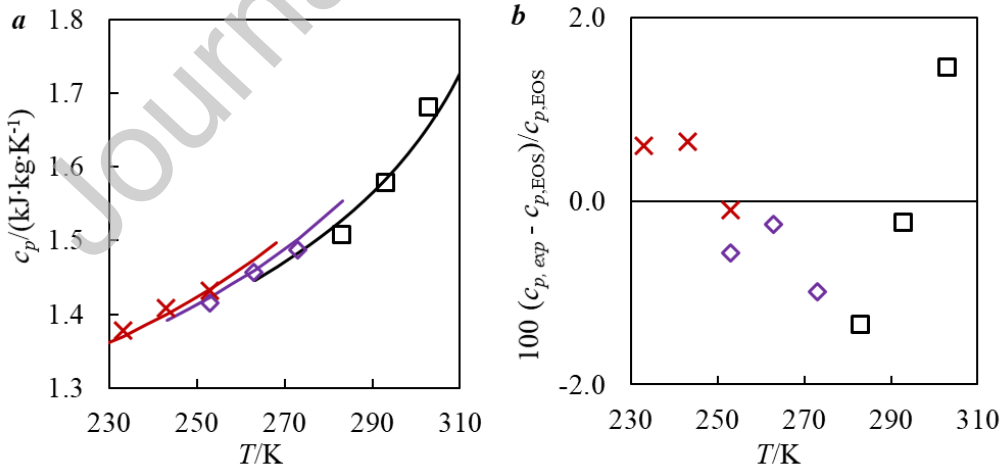

Figure 8. Heat capacity measurements of 0.5 CO_2 + 0.5 R1234yf. *a*: Absolute c_p as a function of T (temperature), symbols correspond to the measured values (□ 5.09 MPa ◇ 3.50 MPa ×2.07 MPa) and the solid coloured lines correspond to the predictions from REFPROP 10[1]. *b*: Relative deviations of the measured c_p (using average fitted cell volume) from that calculated using the default model in REFPROP 10[4] ($c_{p,cal}$) at different pressures (□ 5.09 MPa ◇ 3.50 MPa ×2.07 MPa) as a function of temperature.

Table 8. Heat capacity c_p, and its combined standard uncertainty $u_c(c_p)$ as a function of temperature T and pressure p. At all temperatures, $u(T)$ = 0.2 K, $u(x)$ = 0.005 for binary components, and the $u(x)$ for multi-component mixtures are given in the table..

T/K	p/MPa	$u(p)$/MPa	c_p/ (kJ·kg-1·K-1)	$u_c(c_p)$/(kJ·kg^{-1}·K^{-1})
0.500 CO_2 + 0.500 R32				
272.98	5.00	0.03	1.989	0.036
282.96	5.00	0.03	2.098	0.038
292.93	5.00	0.03	2.257	0.041
253.05	3.52	0.02	1.898	0.034
263.00	3.52	0.02	1.937	0.035
272.98	3.52	0.02	2.013	0.036
223.13	1.50	0.01	1.803	0.033
233.09	1.50	0.01	1.833	0.033
243.06	1.50	0.01	1.871	0.034
0.501 CO_2 + 0.499 R134a				
283.08	5.00	0.03	1.682	0.030
293.02	5.00	0.03	1.744	0.031
303.02	5.00	0.03	1.833	0.033
253.01	3.50	0.02	1.567	0.028
263.00	3.50	0.02	1.581	0.028
233.07	2.00	0.01	1.504	0.027
243.02	2.00	0.01	1.526	0.027
253.02	2.00	0.01	1.567	0.028
0.500 CO_2 + 0.500 R125				
272.99	5.10	0.03	1.531	0.028
282.93	5.10	0.03	1.587	0.029
292.90	4.92	0.03	1.732	0.032
253.04	3.52	0.02	1.440	0.026
263.00	3.52	0.02	1.487	0.027
272.97	3.52	0.02	1.541	0.028
223.13	1.50	0.01	1.352	0.024
233.08	1.58	0.01	1.370	0.025
243.05	1.60	0.01	1.421	0.025
0.499 CO_2 + 0.501 R1234yf				
282.94	5.10	0.03	1.508	0.027
292.92	5.10	0.03	1.579	0.029
302.89	5.08	0.03	1.681	0.031
253.02	3.50	0.02	1.416	0.025
262.99	3.50	0.02	1.456	0.026
272.95	3.50	0.02	1.487	0.027
233.06	2.07	0.01	1.378	0.025
243.04	2.07	0.01	1.409	0.025
253.02	2.07	0.01	1.433	0.026
(0.093 ± 0.010) CO_2 + (0.477 ± 0.008) R1234yf + (0.430 ± 0.008) R32				
302.98	4.50	0.02	1.610	0.030
322.90	4.55	0.02	1.817	0.036
283.04	2.98	0.02	1.502	0.028
293.04	2.98	0.02	1.560	0.029
242.69	1.55	0.01	1.361	0.025
252.64	1.55	0.01	1.379	0.025
(0.200 ± 0.007) CO_2 + (0.200 ± 0.004) R1234yf + (0.200 ± 0.008) R32 + (0.200 ± 0.006) R125 + (0.200 ± 0.006) R134a				
302.79	5.00	0.03	1.564	0.030
322.73	4.90	0.03	1.773	0.035
272.88	3.58	0.02	1.409	0.026
302.80	3.58	0.02	1.531	0.029
252.95	1.50	0.01	1.351	0.025
262.91	1.50	0.01	1.384	0.026

3.2 Modeling

3.2.1 Parameter tuning results

In this work the number of thermodynamic data available for a given binary mixture was limited. Thus, it was only necessary to tune two BIPs from their standard value (unity) to achieve acceptable fits to the data. A summary of binary mixture tuning is shown in Table 9. The results of reviewing the literature for the thermodynamic properties of the refrigerant mixtures investigated in this work are shown in Table 10. Almost all of the reported literature data were included in the new model fitting. Significant improvements were achieved for the mixtures of (R32 + CO_2) and (R134a + CO_2): the RMS deviations decreased for all the properties. For the mixtures of (R125 + CO_2) and (R1234yf + CO_2), the regression mainly been focused on density as the default model was only fit to the VLE data available at the time. For all the mixtures, the heat capacity predictions were insensitive to changes in the BIPs.

Table 9. Overview of the binary interaction parameters from the Helmholtz energy models tuned in this work and implemented as the default in REFPROP 10. The adjustable parameter F_{ij} associated with the departure function was not varied for any binary.

	Default in REFPROP 10					Values after tuning in this work				
System	$\beta_{T,ij}$	$\gamma_{T,ij}$	β_v	$\gamma_{v,ij}$	F_{ij}	$\beta_{T,ij}$	$\gamma_{T,ij}$	$\beta_{v,ij}$	$\gamma_{v,ij}$	F_{ij}
CO_2 + R32	1	0.99782	1	1.0059	0	1	0.992	1	0.9786	0
CO_2 + R134a	1	1.008	1	1	0	1	1	1.016	1.027	0
CO_2 + R125	1.0115	0.96741	1	1	0	1	0.9871	1	1.0311	0
CO_2 + R1234yf	1.017	1	1	1.015	-0.657	1	1	1.125	1.051	-0.657

The quality of the literature VLE data was checked via comparisons of the vapour-liquid equilibrium ratio K_i. As a result, not all the literature data were used in the regression process. In Figure S7 and Figure S9, the tuned models from this work represent the VLE of (CO_2 + R32) and (CO_2 + R125) with small deviations. Fewer outliers can also be observed in the corresponding isotherms. In Figure S8 and Figure S10 of the SI, for the binaries of (CO_2 + R134a) and (CO_2 + R1234yf), the tuned models exhibit the same quality as the default REFPROP 10 models in the isotherms and the deviation plots. For these two mixtures, better performance in VLE was not achieved because the default models were tuned to VLE data only, while in this work, the models were also tuned to density data.

Table 10. Sources of data for mixtures with the type of reported data, the number of measured data (N), the (percentage) RMS deviations between the default and tuned Helmholtz energy mixture models calculated using eqs (12)-(14), and the number of data used for tuning in this work (N_{tuned}).

Reference	Type	N	RMS (default)	N_{tuned}	RMS (tuned)
CO_2 + R32					
Diefenbacher and Türk[36]	VLE	9	0.018	8	0.012
Rivollet et al.[33]	VLE	45	0.018	43	0.008
Stein and Adams [37]	VLE	48	0.009	0	0.019
Di Nicola et al. [38]	VLE	5	0.45	0	0.27
This work	ρ	9	1.08	9	0.15
Di Nicola et al. [38]	ρ	65	1.17	0	0.77
This work	c_p	9	3.20	9	2.90
This work	VLE	5	0.018	4	0.008
CO_2 + R134a					
Duran-Valencia et al.[34]	VLE	27	0.007	27	0.007
Lim et al.[39]	VLE	37	0.026	36	0.024
Silva-Oliver and Galicia-Luna[40]	VLE	23	0.017	23	0.016
This work	ρ	7	1.67	7	0.34
This work	c_p	8	3.94	8	3.80
This work	VLE	5	0.010	5	0.008
CO_2 + R125					
Di Nicola et al. [38]	VLE	5	0.052	3	0.008
Jeong et al. [41]	VLE	19	0.019	15	0.018
This work	ρ	13	1.19	13	0.55
Di Nicola et al. [38]	ρ	65	1.08	65	0.42
This work	c_p	9	1.18	9	2.10
This work	VLE	5	0.031	5	0.010
CO_2 + R1234yf					
Juntarachat et al.[35]	VLE	65	0.028	54	0.032
Di Nicola et al. [42]	VLE	110	0.20	0	0.21
This work	ρ	12	1.38	12	0.18
Di Nicola et al. [42]	ρ	73	0.91	0	1.02
This work	c_p	9	0.83	9	0.84
This work	VLE	5	0.018	5	0.021

Figure S13 to Figure S16 in the SI show that the density measurements are not well-represented by the REFPROP 10 default model. Systematic offsets occur between the measurements and the model mainly due to a lack of available density data for the binary mixtures during the default model's development. In this work, for almost all the measurements, the density RMS deviations are within the experimental uncertainties because density had the highest weighting of all the properties. Significant improvements were achieved with deviations having been reduced from (54 to 87) %.

For the mixture of (CO_2 + R1234yf), the RMS deviation in heat capacity is smaller than the experimental uncertainty (1.8%). A modification in the departure function might significantly decrease the deviations in heat capacity. However, there are not enough data to reliably tune the departure function and all the adjustable parameters (F_{ij}) remains unchanged from the value used in the default model.

3.2.2 Validation of the model

The thermodynamic models were regressed to the binary data detailed above and used without further adjustment to predict the properties of the ternary and five-component mixtures at the measurement conditions. Interaction parameters have been tuned for most of the other binary subsystems by Akasaka (R32 + R1234yf)[43], Al Ghafri et al. (R125 + R1234yf)[7] and Lemmon and Jacobsen (R134a + R125, R134a + R32 and R125 + R32)[44]. For the mixture of (R134a + R1234yf) there are no thermodynamic property data available in the literature to the authors' knowledge and the default BIPs in REFPROP[9] were used. The statistical results of these predictive comparisons are shown in Table 11.

Table 11. Summary for the multi-component mixture comparisons, the number of measured data, the RMS deviations between the default and tuned Helmholtz energy mixture models calculated using Eqs. (12)-(14).

Property	Data points	RMS (default)	RMS (tuned)
Ternary mixture			
ρ	6	1.67	0.85
VLE	8	0.05	0.02
c_p	6	1.15	1.08
Five-component mixture			
ρ	6	0.79	0.42
VLE	3	0.005	0.004
c_p	6	1.65	1.68

Compared with the default parameters set used in REFPROP, the densities predicted for the multi-component mixtures are significantly improved using the tuned BIPs determined in this work. As shown in Table 11, the deviations decrease by 49% and 47% for the ternary and five-component mixtures, respectively. The same applies to the VLE results for the ternary mixture, where the deviations have decreased by 60%. The RMS deviation of the VLE results was calculated by Eq. 12, where the composition of R32 was used as x_1 and y_1. The deviation of the VLE results from the predictions of default Helmholtz energy mixture model with tuned BIPs are shown in Figure 9(a). As can be seen by comparing Figure 6 and Figure 9(b) for the five component mixture, the deviations between the VLE data and the default model

predictions are similar to those between the data and the optimised model. There is not much change in the heat capacity predictions, which reflects the situation for the binary mixtures that this property is relatively insensitive to the change in BIPs over the measured conditions, and it lacks sufficient data to alter the departure functions.

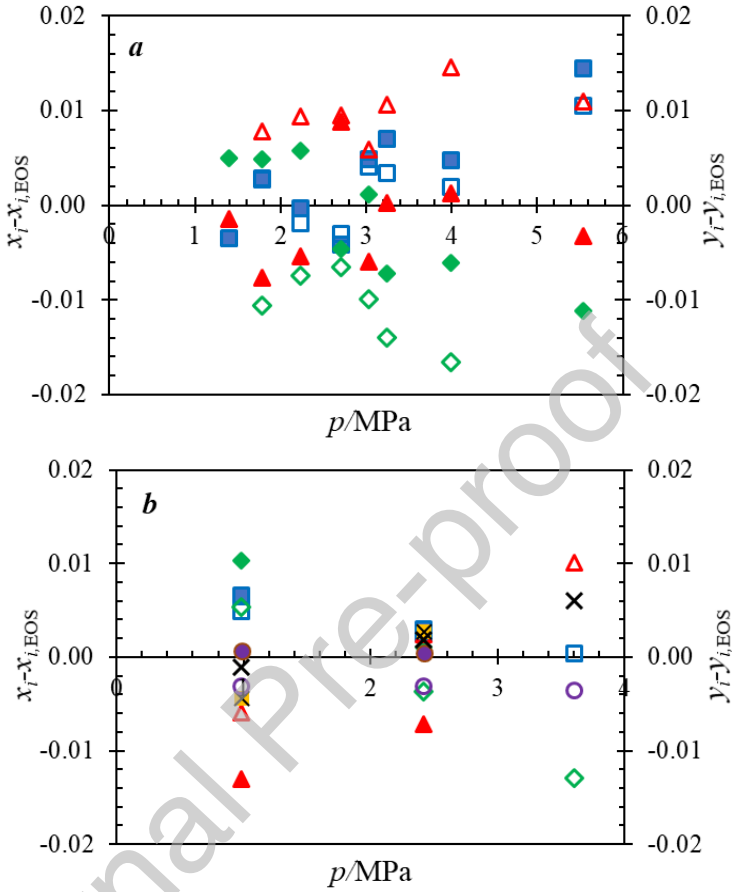

Figure 9. Deviations (x_i-$x_{i,EOS}$) and (y_i-$y_{i,EOS}$) of the measured compositions from those predicted with the Helmholtz energy mixture model using the tuned binary interaction parameters (BIPs) for (*a*) the ternary mixture of (CO_2 + R1234yf + R32) and (*b*) the five-components mixture of [CO_2 + R1234yf + R32 + R125 + R134a]: CO_2 (◆), R1234yf (▲), R32 (■), R125 (●), R134a (☒). Left axis: filled symbols, deviations for liquid; Right axis: empty symbols, deviations for vapour.

4 Conclusion

In this work, we report new data for the thermodynamic properties of carbon dioxide mixtures with HFCs (R32, R125, and R134a) and HFO-1234yf. In summary, we measured:

1. Vapour-liquid equilibria (VLE) for twenty binary mixtures of CO_2 + [R1234yf, R32, R125, R134a] with molar compositions of (10, 20, 30, 50 and 70) % CO_2 measured by the analytic method (sampling with gas chromatography) at 20 °C and pressures from (0.82 to 4.80) MPa.

2. Liquid densities of four equimolar mixtures CO_2 + [R1234yf, R32, R125, R134a] measured by vibrating tube densimetry at temperatures between (-50 and 30) °C and pressures from (1.52 to 5.11) MPa.

3. Liquid heat capacity of four equimolar mixtures CO_2 + [R1234yf, R32, R125, R134a] by differential scanning calorimetry at temperatures between (-50 and 30) °C and pressures between (1.50 and 5.08) MPa.

In addition to the data collected in this work, we also used literature data for VLE, density, and heat capacities to tune the mixture parameters in REFPROP 10 and improve the prediction of these thermodynamics properties. There were significant improvements in the prediction of thermodynamic properties, particularly the density where, for example, the root-mean-square (RMS) of the relative deviation between the model and the experimental data for the (CO_2 + R1234yf) mixture was decreased from (1.38 to 0.18) %. The tuned REFPROP models were then evaluated in terms of their ability to predict the thermodynamic properties of several ternaries and a five-component mixture of HFCs, an HFO, and CO_2. The following mixtures and properties were measured:

1. Vapour-liquid equilibria (VLE) of four ternary mixtures of CO_2 + R1234yf + R32 with respective component compositions of (10, 45, 45) mass%, (20, 40, 40) mass %, (30, 35, 35) mass %, and (50, 25, 25) mass % at T = (10, 40) °C and an equimolar five-component mixture of CO_2 + R1234yf + R32 + R125 + R134a at T = (0, 40, 60) °C.

2. Liquid densities of a ternary mixture of CO_2 + R1234yf + R32, with respective component compositions of (5, 67, 28) mass % and an equimolar five-component mixture of CO_2 + R1234yf + R32 + R125 + R134a at temperatures between (-30 and 50) °C and pressures between (1.43 and 5.07) MPa.

3. Liquid heat capacities of a ternary mixture of CO_2 + R1234yf + R32 , with respective component compositions of (5, 67, 28) mass % and an equimolar five-component mixture of CO_2 + R1234yf + R32 + R125 + R134a at temperatures between (-30 and 50) °C and pressures between (1.50 and 5.00) MPa.

The multi-component mixture measurements showed that the tuned REFPROP models give significantly better predictions of the refrigerant mixtures' thermodynamic properties. Density predictions were improved by a factor of 2. These improved

thermodynamic models will help make simulations of refrigeration processes involving these mixtures more reliable.

Declaration of Competing Interests

The authors declare that they have no known competing financial interests or personal relationships that could have appeared to influence the work reported in this paper.

Acknowledgements

Funding: This work was supported by Mitsubishi Heavy Industries, Ltd.

References

1. Jabbour, T.; Clodic, D. F.; Terry, J.; Kondo, S., Burning velocity and refrigerant flammability classification. *ASHRAE Transactions* **2004,** *110 PART II*, 522-533.

2. Clodic, D.; Jabbour, T., Method of test for burning velocity measurement of flammable gases and results. *HVAC and R Research* **2011,** *17*, 51-75.

3. Bell, I. H.; Domanski, P. A.; McLinden, M. O.; Linteris, G. T., The hunt for nonflammable refrigerant blends to replace R-134a. *International Journal of Refrigeration* **2019,** *104*, 484-495.

4. Bellos, E.; Tzivanidis, C., A comparative study of CO2 refrigeration systems. *Energy Conversion and Management: X* **2019**, *1*, 100002.

5. Wu, X.; Dang, C.; Xu, S.; Hihara, E., State of the art on the flammability of hydrofluoroolefin (HFO) refrigerants. *International Journal of Refrigeration* **2019,** *108*, 209-223.

6. Bobbo, S.; Nicola, G. D.; Zilio, C.; Brown, J. S.; Fedele, L., Low GWP halocarbon refrigerants: A review of thermophysical properties. *International Journal of Refrigeration* **2018,** *90*, 181-201.

7. Al Ghafri, S. Z. S.; Rowland, D.; Akhfash, M.; Arami-Niya, A.; Khamphasith, M.; Xiao, X.; Tsuji, T.; Tanaka, Y.; Seiki, Y.; May, E. F.; Hughes, T. J., Thermodynamic properties of hydrofluoroolefin (R1234yf and R1234ze(E)) refrigerant mixtures: Density, vapour-liquid equilibrium, and heat capacity data and modelling. *International Journal of Refrigeration* **2019,** *98*, 249-260.

8. Akhfash, M.; Al Ghafri, S. Z. S.; Rowland, D.; Hughes, T. J.; Tsuji, T.; Tanaka, Y.; Seiki, Y.; May, E. F., Liquid and Vapor Viscosities of Binary Refrigerant Mixtures Containing R1234yf or R1234ze(E). *Journal of Chemical & Engineering Data* **2019,** *64* (3), 1122-1130.

9. Lemmon, E. W.; Bell, I. H.; Huber, M. L.; McLinden, M. O., NIST Standard Reference Database 23: Reference Fluid Thermodynamic and Transport Properties-REFPROP, Version 10.0, National Institute of Standards and Technology. **2018**.

10. Span, R.; Wagner, W., A new equation of state for carbon dioxide covering the fluid region from the triple‐point temperature to 1100 K at pressures up to 800 MPa. *Journal of physical and chemical reference data* **1996,** *25* (6), 1509-1596.

11. Tillner-Roth, R.; Yokozeki, A., An international standard equation of state for difluoromethane (R-32) for temperatures from the triple point at 136.34 K to 435 K and pressures up to 70 MPa. *Journal of Physical and Chemical Reference Data* **1997,** *26* (6), 1273-1328.

12. Tillner-Roth, R.; Baehr, H. D., An international standard formulation for the thermodynamic properties of 1, 1, 1, 2‐Tetrafluoroethane (HFC‐134a) for temperatures from 170 K to 455 K and pressures up to 70 MPa. *Journal of Physical and Chemical Reference Data* **1994,** *23* (5), 657-729.

13. Lemmon, E. W.; Jacobsen, R. T., A new functional form and new fitting techniques for equations of state with application to pentafluoroethane (HFC-125). *Journal of physical and chemical reference data* **2005,** *34* (1), 69-108.

14. May, E. F.; Guo, J. Y.; Oakley, J. H.; Hughes, T. J.; Graham, B. F.; Marsh, K. N.; Huang, S. H., Reference Quality Vapor–Liquid Equilibrium Data for the Binary Systems Methane + Ethane, + Propane, + Butane, and + 2-Methylpropane, at Temperatures from (203 to 273) K and Pressures to 9 MPa. *Journal of Chemical & Engineering Data* **2015,** *60* (12), 3606-3620.

15. Efika, E. C.; Hoballah, R.; Li, X.; May, E. F.; Nania, M.; Sanchez-Vicente, Y.; Trusler, J. P. M., Saturated phase densities of (CO2 + H2O) at temperatures from (293 to 450) K and pressures up to 64 MPa. *The Journal of Chemical Thermodynamics* **2016,** *93*, 347-359.

16. Guilbot, P.; Valtz, A.; Legendre, H.; Richon, D., Rapid on-line sampler-injector: a reliable tool for HT-HP sampling and on-line GC analysis. *Analusis* **2000,** *28* (5), 426-431.

17. Richon, D. Method and device for taking micro samples from a pressurized fluid contained in a container. Patent FR2853414A1, 2003.

18. Outcalt, S., Calibration Fluids and Calibration Equations: How Choices May Affect the Results of Density Measurements Made with U-Tube Densimeters. *J Res Natl Inst Stand Technol* **2018,** *123*.

19. Jiao, F.; Al Ghafri, S. Z. S.; Hughes, T. J.; May, E. F., Extended calibration of a vibrating tube densimeter and new reference density data for a methane-propane mixture at temperatures from (203 to 423) K and pressures to 35 MPa. *Journal of Molecular Liquids* **2020**, 113219.

20. May, E. F.; Tay, W. J.; Nania, M.; Aleji, A.; Al-Ghafri, S.; Martin Trusler, J. P., Physical Apparatus Parameters and Model for Vibrating Tube Densimeters at Pressures to 140 MPa and Temperatures to 473 K. *Review of Scientific Instruments* **2014,** *85* (9), 095111.

21. Lemmon, E. W.; McLinden, M. O.; Wagner, W., Thermodynamic Properties of Propane. III. A Reference Equation of State for Temperatures from the Melting Line to 650 K and Pressures up to 1000 MPa. *Journal of Chemical & Engineering Data* **2009,** *54* (12), 3141-3180.

22. Setzmann, U.; Wagner, W., A New Equation of State and Tables of Thermodynamic Properties for Methane Covering the Range from the Melting Line to 625 K at Pressures up to 100 MPa. *Journal of Physical and Chemical Reference Data* **1991,** *20* (6), 1061-1155.

23. Joint Committee for Guides in Metrology, JCGM 100:2008 (GUM 1995 with minor corrections), Evaluation of measurement data – Guide to the expression of uncertainty in measurement Paris, 2008.

24. Tay, W. J.; Trusler, J. P. M., Density, sound speed and derived thermophysical properties of *n*-nonane at temperatures between (283.15 and 473.15) K and at pressures up to 390 MPa. *J. Chem. Thermodyn.* **2018,** *124*, 107-122.

25. Syed, T. H.; Hughes, T. J.; Marsh, K. N.; May, E. F., Isobaric Heat Capacity Measurements of Liquid Methane, Ethane, and Propane by Differential Scanning Calorimetry at High Pressures and Low Temperatures. *Journal of Chemical & Engineering Data* **2012,** *57* (12), 3573-3580.

26. Kunz, O.; Wagner, W., The GERG-2008 Wide-Range Equation of State for Natural Gases and Other Mixtures: An Expansion of GERG-2004. *Journal of Chemical & Engineering Data* **2012,** *57* (11), 3032-3091.

27. Kunz, O.; Klimeck, R.; Wagner, W.; Jaeschke, M., The GERG-2004 wide-range equation of state for natural gases and other mixtures. *GERG Tech. Monogr* **2007,** *15*.

28. Span, R.; Lemmon, E. W., CHAPTER 5 Volumetric Properties from Multiparameter Equations of State. In *Volume Properties: Liquids, Solutions and Vapours*, The Royal Society of Chemistry: 2015; pp 125-151.

29. Syed, T. H.; Hughes, T. J.; Marsh, K. N.; May, E. F., Isobaric Heat Capacity Measurements of Liquid Methane + Propane, Methane + Butane, and a Mixed Refrigerant by Differential Scanning Calorimetry at High Pressures and Low Temperatures. *Journal of Chemical & Engineering Data* **2014,** *59* (4), 968-974.

30. Rowland, D.; Hughes, T. J.; May, E. F., Extending the GERG-2008 equation of state: Improved departure function and interaction parameters for (methane+butane). *The Journal of Chemical Thermodynamics* **2016,** *97*, 206-213.

31. Qian, J.-W.; Privat, R.; Jaubert, J.-N.; Coquelet, C.; Ramjugernath, D., Fluid-phase-equilibrium prediction of fluorocompound-containing binary systems with the predictive E-PPR78 model. *International Journal of Refrigeration* **2017,** *73*, 65-90.

32. Jaubert, J.-N.; Coniglio, L., The Group Contribution Concept: A Useful Tool To Correlate Binary Systems and To Predict the Phase Behavior of Multicomponent Systems Involving Supercritical CO2 and Fatty Acids. *Industrial & Engineering Chemistry Research* **1999,** *38* (12), 5011-5018.

33. Rivollet, F.; Chapoy, A.; Coquelet, C.; Richon, D., Vapor–liquid equilibrium data for the carbon dioxide (CO_2) + difluoromethane (R32) system at temperatures from 283.12 to 343.25 K and pressures up to 7.46 MPa. *Fluid Phase Equilibria* **2004,** *218* (1), 95-101.

34. Duran-Valencia, C.; Pointurier, G.; Valtz, A.; Guilbot, P.; Richon, D., Vapor−Liquid Equilibrium (VLE) Data for the Carbon Dioxide (CO_2) + 1,1,1,2-Tetrafluoroethane (R134a) System at Temperatures from 252.95 K to 292.95 K and Pressures up to 2 MPa. *Journal of Chemical & Engineering Data* **2002,** *47* (1), 59-61.

35. Juntarachat, N.; Valtz, A.; Coquelet, C.; Privat, R.; Jaubert, J.-N., Experimental measurements and correlation of vapor–liquid equilibrium and critical data for the CO2 + R1234yf and CO2 + R1234ze(E) binary mixtures. *International Journal of Refrigeration* **2014,** *47*, 141-152.

36. Diefenbacher, A.; Türk, M., (Vapour+liquid) Equilibria of binary mixtures of CO_2, CH_2F_2, CHF_3, and SF_6. *The Journal of Chemical Thermodynamics* **2002,** *34* (9), 1361-1375.

37. Stein, F. P.; Adams, R. A., Vapor-liquid equilibriums for carbon dioxide-difluoromethane system. *J. Chem. Eng. Data* **1971,** *16*, 146-149.

38. Di Nicola, G.; Pacetti, M.; Polonara, F.; Stryjek, R., Isochoric Measurements for CO_2 + R125 and CO_2 + R32 Binary Systems. *Journal of Chemical & Engineering Data* **2002,** *47* (5), 1145-1153.

39. Lim, J. S.; Jin, J. M.; Yoo, K.-P., VLE measurement for binary systems of CO_2+1,1,1,2-tetrafluoroethane (HFC-134a) at high pressures. *The Journal of Supercritical Fluids* **2008,** *44* (3), 279-283.

40. Silva-Oliver, G.; Galicia-Luna, L. A., Vapor–liquid equilibria for carbon dioxide + 1,1,1,2-tetrafluoroethane (R-134a) systems at temperatures from 329 to 354 K and pressures upto 7.37 MPa. *Fluid Phase Equilibria* **2002,** *199* (1), 213-222.

41. Jeong, K.; Im, J.; Lee, S.; Kim, H., (Vapour+liquid) equilibria of the {carbon dioxide+pentafluoroethane (HFC-125)} system and the {carbon dioxide+dodecafluoro-2-methylpentan-3-one (NOVEC™1230)} system. *The Journal of Chemical Thermodynamics* **2007,** *39* (4), 531-535.

42. Di Nicola, G.; Di Nicola, C.; Arteconi, A.; Stryjek, R., PVTx measurements of the carbon dioxide+ 2, 3, 3, 3-Tetrafluoroprop-1-ene binary system. *J. Chem. Eng. Data* **2012,** *57*, 450-455.

43. Akasaka, R., Thermodynamic property models for the difluoromethane (R-32)+ trans-1, 3, 3, 3-tetrafluoropropene (R-1234ze (E)) and difluoromethane+ 2, 3, 3, 3-tetrafluoropropene (R-1234yf) mixtures. *Fluid Phase Equilib.* **2013,** *358*, 98-104.

44. Lemmon, E. W.; Jacobsen, R. T., Equations of state for mixtures of R-32, R-125, R-134a, R-143a, and R-152a. *Journal of physical and chemical reference data* **2004,** *33* (2), 593-620.